Synthesis, characterization and the cytotoxic activity studies of new N_4O complexes derived from 2-((3-(2-morpholinoethylamino)-N3-((pyridine-2-yl)methyl) propylimino) methyl)phenol

Majid Rezaeivala[a,*], Musa Ahmadi[b], Burjor Captain[b], Serap Şahin-Bölükbaşı[c], Ahmad Ali Dehghani-Firouzabadi[d], Robert William Gable[e]

[a] *Department of Chemical Engineering, Hamedan University of Technology, Hamedan 65155, Iran*

[b] *Department of Chemistry, University of Miami, Coral Gables, FL 33124, United States*

[c] *Department of Biochemistry, Faculty of Pharmacy, Sivas Cumhuriyet University, 58140, Sivas, Turkey*

[d] *Department of Chemistry, Faculty of Science, Yazd University, 89195-741 Yazd, Iran*

[e] *School of Chemistry, University of Melbourne, Victoria 3010, Australia*

Corresponding Author email address: mrezaeivala@gmail.com

A new unsymmetrical five-coordinate Schiff base ligand (HL) with an N_4O donor set (**2**), has been prepared by condensation of N1-(2-morpholinoethyl)-N1-((pyridine-2-yl)methyl)propane-1,3-diamine with 2-hydroxy-benzaldehyde. Metal complexes $[ML]^{n+}$ (M = Zn^{2+}, Cd^{2+}, Mn^{2+}, Cu^{2+}, Ni^{2+}, Ag^{+}, Fe^{3+} and Co^{2+} (**3-10**) were synthesized by the reaction of the ligand and metal salts in ethanol. The resulting products were characterized by elemental analyses, IR, ^{1}H and ^{13}C NMR spectra (in the case of Cd and Zn complexes), UV-Vis, ESI-MS and conductivity measurements. The structure of the complexes $[ZnL](ClO_4)$ (**3**), $[CdL](ClO_4)$ (**4**) and $[CuL](ClO_4)$ (**7**) have been determined by single-crystal X-ray diffraction analysis. The metal

complexes were determined to have a distorted trigonal bipyramidal (Zn and Cd) or a distorted square pyramidal (Cu) geometry. The cytotoxic potential of each compound **(1-10)** against MCF-7, MDA-MB-231(breast cancer cells) and PC-3 (prostate cancer cells), as well as WI-38 human normal lung fibroblast cells was evaluated using the MTT assay. Compounds **1, 2** and **10** did not display any activity toward any cell line tested. None of the compounds except compound **8** were cytotoxic towards PC-3. Compounds **4** and **8** showed the highest cytotoxic activity against the MCF-7 and MDA-MB-231 cell lines. Since compounds **3, 6** and **9** have similar IC_{50} values against cancer cells and normal cells, these compounds displayed poor selectivity between cancer and normal cells. More importantly; it was observed that compound **5** acts differently towards different types of cell lines. For example, it displays lower cytotoxicity against the WI-38 normal cell line than it does against the MDA-MB-231 cell line.

Keywords: Morpholine; Schiff base; Unsymmetrical tripodal amine; X-ray; Cytotoxicity.

1. Introduction

Schiff bases have played an important role in the development of coordination chemistry as they easily form stable complexes with most of the transition metals[1]. They show interesting properties, e.g. the ability to reversibly bind oxygen[2], catalytic activity in hydrogenation of olefins[3], photochromic properties[4] and complexing ability towards toxic metals[5].The heterocyclic N, O donor Schiff base ligands have been important in coordination chemistry[6, 7]. Morpholine is a heterocyclic organic compound that has features of both amines and ethers. It has also been produced by the reaction of diethylene glycol and ammonia[8]. This compound is used in the preparation of enantiomerically pure α-amino acids, β-amino alcohols and peptides as a starting material [9], as well as in the manufacture of solvents (e.g. in waxes and polishes),

rubber additives, bactericides, dyes, corrosion inhibitors, crop protection agents, emulsifiers, anti-oxidants, catalysts, optical brighteners, pharmaceutical products and resin industries [10, 11]. Schiff base compounds derived from morpholine are completely stable in biological systems, allowing rigorous long-term application; therefore, they are attracting increasing attention in the design of ligands and their metal complexes for their potential anticancer applications[12]. Many morpholine derivatives display antibacterial[13-16], anticancer[9], antimicrobial[17], antidiabetic[18], anticholinergic [18] and anti-inflammatory[19] activities. Schiff bases of 4-(4-aminophenyl)-morpholine also possess potent antimicrobial activities[20, 21]. It has also been shown that some compounds with the morpholine ring bearing the ethanolamine side chain have been found to possess good adrenergic potential[22, 23]. Dhahagani et al, found it was worthwhile to pursue the synthesis of metal complexes of Schiff base-morpholine ligands in order to develop more potent derivatives. The ligands and their metal complexes were screened for their biopotency anticancer activity in human heptocarcinoma cells. The preliminary bioassay these compounds exhibit inhibitory activity against the human gastric cancer cell lines[17]. Recently, Ohui et al. reported six morpholine-(iso)thiosemicarbazone hybrids and their Cu(II) complexes with good-to moderate solubility and stability in water. The Cu(II) complexes displayed higher antiproliferative activity in cancer cells than triapine[24]. The results of our previous research on the biological activities of Schiff base complexes having piperazine and homopiperazine groups, with either pyridine or non-pyridine moieties[25, 26], as well as our synthesis of new amines and complexes containing the morpholine group[14, 15, 27-29], have motivated us to explore the synthesis and cytotoxicity of a new penta-dentate Schiff base ligand (**2**) and its metal complexes [ZnL](ClO_4) (**3**), [CdL](ClO_4) (**4**), [MnL](ClO_4) (**5**), [NiL](ClO_4) (**6**), [CuL](ClO_4) (**7**), [AgHL(NO_3)] (**8**), [$FeLCl_2$] (**9**) and [CoL](ClO_4) (**10**). The coordination behaviour of the Schiff

bases towards transition metal ions were examined using appropriate physico-chemical techniques. The cytotoxic activities of the amine, the synthesized ligand and its complexes (**1-10**) were determined using MTT (3-(4,5-dimethylthiazol-2-yl)-2,5-diphenyl tetrazolium bromide) assay on MCF-7, MDA-MB-231 and PC-3 cancer cells, as well as on WI-38 human normal lung fibroblast cells.

2. Experimental

General remarks

2-Hydroxybenzaldehyde, 2-morpholinoethanamine, and metal salts were purchased from Aldrich and used without purification. Infrared spectra (IR) were collected on a BIO-RAD FTS-40A spectrophotometer (4000-400 cm^{-1}). Nuclear magnetic resonance (NMR) spectra were recorded on a Bruker 400 and 500 spectrometer operating at 399.993 and 500.06 MHz, respectively. Electrospray mass spectrometric (ESI-MS) measurements were obtained on a Bruker micro TOF-QII at University of Miami Coral Gables, FL. UV-Vis analyses were carried out on a Shimadzu Model UV-2600 system. Standard microanalysis for all complexes was carried out using a Perkin-Elmer, CHNS/O Elemental analyser model 2400. Conductivity measurements were carried out in 10^{-3} mol dm^{-3} MeCN solutions at 20 °C using a CARISON GLP32 conductivity meter.

2.1. X-ray analysis

Single crystals of **3, 4** and **7** suitable for diffraction analysis were grown by slow evaporation of the solvent from an acetonitrile/ethanol solution at room temperature. The crystals were glued onto the end of thin glass fiber. X-ray intensity data were measured on a Bruker SMART APEX2 CCD-based diffractometer using Mo Kα radiation (λ = 0.71073 Å)[29]. The raw data frames were

integrated with the SAINT+ program using a narrow-frame integration algorithm[29]; corrections for Lorentz and polarization effects were also applied with SAINT+. An empirical absorption correction based on the multiple measurements of equivalent reflections was applied using the program SADABS. All structures were solved by a combination of direct methods and difference Fourier syntheses and refined by full-matrix least-squares on F^2, by using the SHELXTL software package [30, 31]. All non-hydrogen atoms were refined with anisotropic displacement parameters. Hydrogen atoms were placed in geometrically idealized positions and included as standard riding atoms during the least-squares refinements. Crystal data, data collection parameters, and results of the analyses are listed in Table 1. All three complexes crystallized in the orthorhombic crystal system. The systematic absences in the intensity data were consistent with the unique space group $P2_12_12_1$.

Table 1 here

2.2. Synthesis of N1-(2-morpholinoethyl)-N1-((pyridine-2-yl)methyl)propane-1,3-diamine *(1)*

The amine was prepared according to literature methods[32, 33]. A solution of 2-morpholinoethanamine (1.30 g, 10 mmol) in dry EtOH (30 mL) was added dropwise to a warm solution of pyridine-2-carbaldehyde (2.14 g, 20.0 mmol) in dry EtOH (30 mL) over 2 h. The mixture was refluxed while stirring for 12 h and then allowed to cool to room temperature. Solid sodium borohydride (3.78 g, 100 mmol) was then added slowly and the reaction mixture was heated at reflux for further 2 h. The solution was filtered and the filtrate volume decreased to 20 mL by rotary evaporation. Water (50 ml) was added and the product was extracted with

chloroform (3 × 25 mL); the organic layers were all combined together and dried over magnesium sulfate. The chloroform was removed by rotary evaporation to leave a yellow oil. The resulting product (10 mmol) was dissolved in acetonitrile (20 mL), and K_2CO_3 (2.76 g, 20 mmol) was added. The mixture was refluxed and then a solution of N-(3-bromopropyl)phthalimide (3.22 g, 12.0 mmol) in acetonitrile (40 mL) was added. The mixture was refluxed for 24 h and then filtered hot. The solvent was removed by rotary evaporation. The resulting product was boiled under reflux for 20 h in aqueous HCl (25%, 100 mL). After this time the volume was reduced to ca. 25 mL under vacuum and cooled in a refrigerator for several hours. The precipitate was filtered off, and the filtrate was removed under vacuum. Water (50 mL) was added to the mixture and the pH was adjusted to 12 with the addition of a solution of 2M sodium hydroxide. The product was extracted with chloroform (3×25 mL), and then the organic layes were all combined together, and dried over magnesium sulfate. The chloroform was removed by rotary evaporation to leave the product as a brown oil (Scheme 1). Yield: (70%). Anal. Calc. for $C_{15}H_{26}N_4O$ (M. W. 278.39) : C, 64.71; H, 9.41; N, 20.13 Found: 64.90; H, 9.32; N, 20.33. ESI-MS (m/z, %): 279.01 (100%) $(L+1)^+$. ^{1}H NMR (DMSO, ppm) δ = 1.68 (p, 2H, H-f); 2.40 (b, 4H, H-b); 2.48 (t, 2H, H-e); 2.60 (t, 2H, H-d); 2.65 (t, 2H, H-c); 2.68 (b, 2H, H-h); 2.81 (t, 2H, H-g); 3.69 (t, 4H, H-a); 3.75 (s, 2H, H-i); 7.17 (t, 1H, H-m); 7.40 (d, 1H, H-k); 7.60 (t, 1H, H-l); 8.55 (d, 1H, H-n). ^{13}C NMR (DMSO, ppm) δ = 51.00 (c-f); 51.89 (c-g); 53.99 (c-b); 56.50 (c-c, c-d); 60.38 (c-e); 66.66 (c-a); 79.57 (c-i); 122.44(c-m); 123.23 (c-k'); 136.81 (c-l); 149.08 (c-n), 160.29 (c-j).

2.3. Synthesis of 2-((3-(2-morpholinoethylamino)-N3-((pyridine-2-yl)methyl) propylimino)methyl) phenol (HL)(2)

N1-(2-morpholinoethyl)-N1-((pyridine-2-yl)methyl)propane-1,3-diamine (0.5 mmol, 0.139 g) in

ethanol (20 mL) was added dropwise to a solution of 2-hydroxybenzaldehyde (0.5 mmol, 0.061 g) in ethanol (50 mL), while stirring. The mixture was refluxed while stirring for 12 h. After cooling to room temperature, a brown oil was obtained. The supernatant liquid was decanted and the oil was washed with cold ethanol and dried in vacuo.Yield: (75%). Anal. Calc. for $C_{22}H_{30}N_4O_2$ (M. W. 382.49): C, 69.08; H, 7.94; N, 14.65. Found: C, 69.60; H, 7.02; N, 14.82%. ESI-MS (m/z, %): 382.40 (100%) $[HL]^+$. ^{1}H NMR ($CDCl_3$, ppm) δ = 1.86 (b, 2H, H-f'); 2.38 (t, 4H, H-b'); 2.46 (t, 2H, H-e'); 2.61 (t, 2H, H-c'); 2.67 (t, 2H, H-d'); 3.58 (t, 2H, H-g'); 3.64 (t, 4H, H-a'); 3.76 (s, 2H, H-i'); 6.83 (t, 1H, H-s'); 6.91 (d, 1H, H-p'); 7.10 (t, 1H, H-m'); 7.18 (t, 1H, H-k'); 7.26 (t, 1H, H-r'); 7.43 (t, 1H, H-q'); 7.59 (t, 1H, H-l'); 8.28 (s, 1H, H-h'); 8.48 (d, 1H, H-n'); 12.96 (b, 1H, H-u'). ^{13}C NMR ($CDCl_3$, ppm) δ = 28.43 (c-f'); 51.41 (c-e'); 52.11 (c-c'); 54.04 (c-b'); 56.91 (c-d'); 57.27 (c-g'); 60.88 (c-i'); 66.89 (c-a'); 116.97(c-s'); 118.41 (c-m'); 118.70 (c-q'); 121.89 (c-k'); 122.85 (c-o'); 131.07 (c-r'); 132.07 (c-p'); 136.34 (c-l'); 148.92 (c-n'); 160.02 (c-h'); 161.21 (c-j'); 164.88(c-t') (Scheme 1). UV-Vis in CH_3CN (λ, nm) 211 (logε =5.30), 255 (logε = 5.00), 316 (logε = 4.47).

Scheme 1 here

2.4. General synthesis of the metal complexes (3-10)

A solution of ligand, (**2**) (0.191 g, 0.50 mmol) in ethanol (50 mL) was added dropwise to a hot solution of the selected metal salts, $M(ClO_4)_2.xH_2O$ (M = Zn, Cd, Mn, Ni, Cu, Co), $AgNO_3$ and $FeCl_3.6H_2O$ (0.50 mmol). The solution was refluxed for 12 h and then was concentrated under reduced pressure to ca. 5-10 mL. The complexes were filtered off, washed with cold ethanol and dried under vacuum. Crystalline compounds (**3** and **4**) were obtained by slow evaporation of the solvent from an acetonitrile/ethanol or acetonitrile/methanol), respectively. Single crystals of **7** were obtained by slow diffusion of diethyl ether vapour into a solution of this compound in acetonitrile/ethanol at room temperature.

[ZnL](ClO$_4$) (3)

Yield: (0.177 g, 65%). Anal. Calc. for $C_{22}H_{29}ClN_4O_6Zn$ (M. W. 546.3219): C, 48.37; H, 5.35; N, 10.26. Found: C, 48.57; H, 5.20; N, 10.58%. ESI-MS (m/z, %): 445.1609 (100%) $[ZnL]^+$. UV-Vis in CH_3CN (λ, nm) 223 (logε = 5.22), 242 (logε = 5.20), 264 (logε = 4.84), 372 (logε = 4.64). Λ_m (CH_3CN) =202 $\Omega^{-1}cm^2$ mol^{-1}. ^{1}H NMR (CD_3CN, ppm) δ = 1.93 (p, 2H, H-f); 2.17 (s, 2H, H-i); 2.63 (t, 2H, H-e); 2.65 (t, 2H, H-g); 3.18 (t, 2H, H-h-d); 3.24 (t, 2H, H-c); 3.85 (d, 1H, H-a-α); 3.97 (d, 1H, H-b-α); 4.01 (d, 1H, H-b-β); 4.31 (d,1H, Ha-β), 6.53 (t,1H, H-q); 6.86 (d, 1H, H-p); 7.15 (d, 1H, H-s); 7.29 (t, 1H, H-r); 7.51 (d, 1H, H-k); 8.04 (t, 1H, H-l); 8.25 (s, 1H, H-h); 8.56 (t, 1H, H-m); 9.02 (d, 1H, H-n). ^{13}C NMR (CD_3CN, ppm) δ = 26.69 (c-f'); 51.67 (c-e', c-c'); 56.40 (c-b'); 57.95 (c-d', g', i'); 63.63 (c-a'); 113.85 (c-s); 118.36 (c-m); 122.48 (c-q); 124.56(c-k); 124.73 (c-o); 134.79 (c-r); 135.93 (c-p); 140.96 (c-l); 148.96 (c-n); 155.50 (c-h); 170.48 (c-j); 172.73 (c-t).

[CdL](ClO$_4$) (4)

Yield: (0.213 g, 72%). Anal. Calc. for $C_{22}H_{29}CdClN_4O_6$ (M. W. 593.3529): C, 44.53; H, 4.93; N, 9.44. Found: C, 44.73; H, 4.85; N, 9.64 %. ESI-MS (m/z, %): 495.1357 (100 %) $[CdL]^+$. UV-Vis in CH_3CN (λ, nm) 212 (logε = 5.00), 243 (logε = 5.00), 262 (logε = 4.61), 371 (logε = 4.40). Λ_m (CH_3CN) =170 $\Omega^{-1}cm^2$ mol^{-1}.

^{1}H NMR ($CDCl_3$, ppm) δ = 1.94 (p, 2H, H-f'); 2.22 (s, 2H, H-i); 2.56 (t, 2H, H-e); 2.69 (t, 2H, H-g); 3.17 (t, 2H, H-d); 3.62 (t, 2H, H-c); 3.74 (d, 1H, H- a-α); 3.89 (d, 1H, H-b-α); 4.04 (d, H b-β); 4.21 (d, H a-β); 6.51 (t, 1H, H-m); 6.76 (d, 1H, H-k); 7.10 (d, 1H, H-p); 7.21 (t, 1H, H-r); 7.53 (t, 2H, H-q,r); 8.02 (t, 1H, H-l); 8.16 (s, 1H, H-h); 8.55 (d, 1H, H-n). ^{13}C NMR ($CDCl_3$, ppm) δ=27.37 (c-f'); 51.17 (c-e'); 56.53 (c-d'); 58.29 (c-g'); 63.72 (c-i'); 65.10 (c-a'); 113.44(c-

s'); 116.90 (c-m'); 118.84 (c-q'); 123.63 (c-k'); 124.92 (c-o'); 125.42 (c-r'); 133.79 (c-p'); 136.85 (c-l'); 140.58 (c-n'); 148.48 (c-h'); 155.44 (c-j'); 172.06 (c-t').

[MnL](ClO$_4$) (5)

Yield: (0.185 g, 69%). Anal. Calc. for $C_{22}H_{29}ClMnN_4O_6$ (M. W. 535.8799): C, 49.31; H, 5.45; N, 10.46. Found: C, 49.25; H, 5.62; N, 10.38 %. ESI-MS (m/z, %): 436.1675(100%) $[MnL]^+$. UV-Vis in CH_3CN (λ, nm) 203 (logε = 5.31), 231 (logε = 5.22), 262 (logε = 5.05), 365 (logε = 4.44). Λ_m (CH_3CN) =160 $\Omega^{-1}cm^2$ mol^{-1}.

[NiL](ClO$_4$) (6)

Yield: (0.172 g, 64%). Anal. Calc. for $C_{22}H_{29}ClN_4NiO_6$ (M. W. 539.6353): C, 48.97; H, 5.42; N, 10.38. Found: C, 49.22; H, 5.33; N, 10.49 %. ESI-MS (m/z, %): 439.1603 (100 %) $[NiL]^+$. UV-Vis in CH_3CN (λ, nm) 213 (logε = 4.66), 226 (logε = 4.74), 241 (logε = 4.65), 372 (logε = 3.97), 479 (logε = 2.81). Λ_m (CH_3CN) =207 $\Omega^{-1}cm^2$ mol^{-1}.

[CuL](ClO$_4$) (7)

Yield: (0.199 g, 73%). Anal. Calc. for $C_{22}H_{29}ClCuN_4O_6$ (M. W. 544.4879): C, 48.53; H, 5.37; N, 10.29. Found: C, 48.39; H, 5.54; N, 10.16 %. ESI-MS (m/z, %): 444.1626 (100%) $[CuL]^+$. UV-Vis in CH_3CN (λ, nm) 222 (logε = 4.92), 243 (logε = 4.83), 268 (logε = 4.73), 316 (logε = 4.15), 370 (logε = 4.14), 464 (logε = 2.51), 622 (logε = 2.45). Λ_m (CH_3CN) =152 $\Omega^{-1}cm^2$ mol^{-1}.

[AgHL(NO$_3$)] (8)

Yield: (0.386 g, 70%). Anal. Calc. for $C_{22}H_{30}AgN_5O_5$ (M. W. 552.3723): C, 47.92; H, 5.30; N,

12.70. Found: C, 48.43; H, 5.48; N, 12.59 %. ESI-MS (m/z, %): 489.1450 (100 %) $[AgHL]^+$. UV-Vis in CH_3CN (λ, nm) 204 (logε = 5.30), 253 (logε = 4.98), 316 (logε = 4.41). Λ_m (CH_3CN) =136 $\Omega^{-1}cm^2\ mol^{-1}$.

[FeLCl_2] (9)

Yield: (0.165 g, 65%). Anal. Calc. for $C_{22}H_{29}Cl_2FeN_4O_2$ (M. W. 507.1017): C, 51.99; H, 5.75; N, 11.02. Found: C, 51.82; H, 5.95; N, 10.93 %. ESI-MS (m/z, %): 472.1360 (100 %) $[FeL]Cl^+$. UV-Vis in CH_3CN (λ, nm) 202 (logε = 5.00), 240 (logε = 4.71), 261 (logε = 4.53), 311 (logε = 4.41), 361 (logε = 4.43). Λ_m (CH_3CN) =43 $\Omega^{-1}cm^2\ mol^{-1}$.

[CoL](ClO_4) (10)

Yield: (0.188 g, 70%). Anal. Calc. for $C_{22}H_{29}ClCoN_4O_6$ (M. W. 539.8751): C, 48.94; H, 5.41; N, 10.38. Found: C, 48.82; H, 5.75; N, 10.29 %. ESI-MS (m/z, %): 440.1626 (100%) $[CoL]^+$. UV-Vis in CH_3CN (λ, nm) 217 (logε = 5.10), 251 (logε = 5.05), 376 (logε = 4.08), 466 (logε = 3.45). Λ_m (CH_3CN) =168 $\Omega^{-1}cm^2\ mol^{-1}$.

2.5. Cytotoxic activity

2.5.1. Cell culture

The human cancer cell lines MCF-7 (HTB-22, human breast adenocarcinoma cells expressing estrogen receptors, ER+, progesterone receptors, PR+, human epidermal growth factor receptor 2, HER2+), MDA-MB-231 (HTB-26, human breast adenocarcinoma cells, triple-negative cells which do not express human epidermal growth factor receptor 2 (HER2), HER2-, estrogen receptors, ER-, and progesterone receptors, PR-), PC-3 (CRL-1435, human prostate adenocarcinoma cells which are androgen insensitive, have high metastatic potential and also do

not express p53 genes), WI-38 (CCL-75, human normal lung fibroblast cells), F-12K Medium (30-2004), Eagles Minimum Essential Medium (EMEM, 30-2003), fetal bovine serum (FBS, 30-2020) and penicillin and streptomycin (30-2300) were purchased from American Type Culture Collection (ATCC, Manassas, VA). Dulbecco's Modified Eagle's Medium (DMEM, D6429), MTT ((3-(4,5-dimethylthiazol-2-yl)-2,5-diphenyltetrazolium bromide) ((M-2128) and Trypsin-EDTA solution (T-3924) were purchased from Sigma Aldrich (Sigma-Aldrich Chemie GmbH , Steinheim, Deutschland).

2.5.2. The MTT assay

The MTT method was used to determine the cytotoxic activity of compounds **1-10** [34]. PC-3 and WI-38 cell lines were cultured in Kaighn's Modification of Ham's F-12 Medium (F-12) and Eagle's Minimum Essential Medium (EMEM) medium, respectively. MCF-7 and MDA-MB-231, were cultured in the Dulbecco's Modified Eagle's Medium (DMEM) medium. The cells were cultured in an incubator with 5% CO_2 and 95 % air in a humidified atmosphere at 37 °C. All media were supplemented with 10% FBS and 1% penicillin/streptomycin solution. When the cells confluence reached 80% or higher, cells were passaged and seeded in a 96-well plate at a density of 1×10^5 cells/well and allowed to adhere to the good walls for 24 hours at 37 °C in a 5% CO_2 and 95 % air in a humidified incubator. Compounds were dissolved in DMSO and diluted with cell culture media to the desired concentrations. 1 µl of each concentration (10-100 µM) of the compounds was added to each well. Control and negative control wells were treated with culture medium and sterile DMSO. After 72 h, 10 µl of the MTT solution was added to each well and the cells were allowed to incubate at 37 ºC for further 2h, after which the media was completely removed. After DMSO was added to each well to dissolve the stain, plates were incubated for 15 min at room temperature. Finally, optical density was measured at 570 nm an

ELISA (Biotek, Epoch, USA). All experiments of this study were carried out in triplicate. Data represented the average values of nine independent measurements with standard error means (±SEM).

2.5.3. Statistical analysis

All cytotoxic activity experiments were carried out in triplicate and results are expressed as means ± SE. Data were analyzed using the one-way analysis of variance, and differences were considered significant at *$p < 0.05$, **$p < 0.005$, ***$p < 0.0005$, ****$p < 0.0001$. The IC_{50} values were determined using statistical software, GraphPad Prism7 (GraphPad Software, San Diego, CA, USA).

3. Results and Discussion

3.1. Syntheses and structural characterization of complexes

An unsymmetrical tripodal amine, (**1**), was prepared in high yield (70%). Subsequently, a one-pot reaction of this amine with 2-hydroxybenzaldehyde was employed to generate a new Schiff-base ligand, (**2**) (Scheme 1). The complexes were prepared from 1:1 ratio reaction between HL and metal salts in ethanol. Crystallization of these compounds has been detailed in the experimental section. Three single crystals were obtained in good yields (64-73%).

3.2. Conductance measurements

Conductivity measurements in non-aqueous solutions have frequently been used in structural studies of metal chelates within the limits of their solubility[16]. It was concluded from the obtained results that the molar conductance values of the Zn(II), Mn(II), Cd(II), Ni(II), Cu(II) and Ag(I) complexes fall in the range (136-202) $\Omega^{-1}mol^{-1}cm^{2}$. It is obvious from these data that

these chelates are ionic in nature and are 1:1- type electrolytes[35], although some data are higher than reported for this type of electrolyte[36]. The conductance value of the Fe(III) complex is 43 $\Omega^{-1}mol^{-1}cm^2$ indicating that this complex is a non-electrolyte[35] and that the chloride ions are coordinating to the metal [35].

3.3. FT- IR spectra

To understand the binding mode of the ligand to the corresponding metal ions, infrared spectral data of HL and their related metal complexes have been compared. The coordination of the ligand to the corresponding metal ion was confirmed on the basis of shifts in absoprtion bands of various groups and absence of certain absorptions (Table 2). The spectrum of the free Schiff base ligand (**2**) shows a band in 1632 cm^{-1} characteristic of the ν (C=N) stretching mode, indicating the successful formation of the ligand, HL[37]. Except for the Ag(I) complex, a comparison of the IR spectral data of ligands and the metal complexes reveals that the band corresponding to ν (C=N) vibration shifts to lower frequency (1617-1622) cm^{-1}, which indicates the involvement of the nitrogen of azomethine in metal complexation[16, 38] [39, 40], This is further supported by the appearance of a new band at 571-593 cm^{-1} due to ν (M-N) stretching vibrations [41]. The ν (C=N) for the Ag(I) complex is found at 1633 cm^{-1} suggesting that the nitrogen of the azomethine group is weakly coordinated. The complex [AgHL(NO_3)] shows two bands at 1033 cm^{-1} and at 1372 cm^{-1}, which may be assigned to the asymmetric and symmetric stretches υ_1 and υ_2 of the nitrate group, suggesting that the NO_3^- group is coordinating to the silver in a monodentate fashion [42-44]. A search of the CSD found eight silver complexes with coordinating nitrate, with four, five or six coordination, and with both chelating and bridging nitrate ligands; all polymeric. This leads to a number of possible structures for [AgHL(NO_3)], both monomers and polymers, with 4,

5 or 6 coordination; the complex dissociates in solution to form $[AgHL]^+$ and $(NO_3)^-$ ions indicating that the nitrate ions are weakly bound to the Ag^+ ions[45]. Besides, the presence of a band for hydroxyl group (OH) at 3448 cm^{-1} and lack of corresponding M-O band indicates that the hydroxyl group is not deprotonated on the Ag complex. Therefore, it is believed that the Ag ions coordinated to four atoms including nitrogen of azomethine, the nitrogen of morpholine, the tertiary nitrogen and an oxygen atom from a monodentate nitrate ion.

Absorptions attributable to the perchlorate ions are seen at approximately 1088-1090 and 624-626 cm^{-1}, the lack of splitting for these bands suggests that the perchlorate anions are not coordinated to the metal[46, 47].

Table (2) here

3.4. Mass spectra

The ESI mass spectra of **1** and **2** show well-defined molecular ion peaks at m/z 279.04 and 382.40, respectively (SI-1, 2), which is consistent with the formation of these compounds. The structures of the complexes in solution were also examined by ESI-MS. For example, the measured m/z value and the isotope distribution pattern of Ag and Fe complexes agree well with the corresponding simulated ones, indicating that each complex keeps its mononuclear structure and oxidation state in solution (SI 9,10, 12,13) [48]. For each complex the molecular ion peak corresponds to the metal complex cation indicating that ClO_4^- is not coordinated in solution, which is consistent we the information we get from FT-IR (SI-3-14).

3.5. UV-Visible spectra

The nature of the ligand field around the metal ion was inferred from the electronic spectra. The electronic spectrum for 0.005 M solutions of the ligand (**2**) (SI-15) in CH_3CN shows three

absorption bands at 211 nm (logε = 5.30), 255 nm (logε = 5.00) and 316 nm (logε = 4.47), which can be attributed to n→σ*, π→π* and n→π* transitions, respectively. The electronic spectra for 0.005 M solutions of complexes (SI-16-23) in CH_3CN show bands at 202-223 nm corresponding to n → σ* transitions originating from the azomethine function of the Schiff base ligand[49] and bands at 231-268 nm corresponding π→π* transitions bands at 311-376 nm corresponding to n→π* and/or charge transfer transitions. The changes in both the position and intensity of the n→σ* and n→π* bands for metal complexes compared to the ligand (**2**) confirm the formation of metal complexes. In general, the electronic d→d transitions for Zn(II), Cd(II), Ag(I) (d^{10}) and Mn(II), Fe(III) (d^5 high spin) complexes are spin-forbidden; hence no bands associated with these transitions can be observed. Copper (II) complex with C_{4v} symmetry are expected to have three d-d transitions: $^2B_1 \rightarrow {}^2A_1$, $^2B_1 \rightarrow {}^2B_2$, and $^2B_1 \rightarrow {}^2E_1$. These transitions are observed at 370 nm (logε = 4.14) (overlapping with a charge transfer band), 464 nm (logε = 2.51) and 622 nm (logε = 2.45). The cobalt (II) complex exhibits absorption peaks at 376 nm (logε = 4.08) (overlapping with a charge transfer band) and 466 nm (logε = 3.45) suggesting five-coordinate geometry for this complex[50]. The electronic spectrum of the Ni(II) complex (**6**) shows the presence of two bands at 372 nm (logε = 3.97) and 479 nm (logε = 2.81). The first band is assigned to a charge transfer transition while the second bond is a band is attributed to a d–d transition in this high-spin five-coordinate complex[51].

3.6. NMR studies

The ^1H NMR spectrum of N1-(2-morpholinoethyl)-N1-((pyridine-2-yl)methyl)propane-1,3-diamine (SI-24) shows a significant signal at 2.68 ppm corresponding to the NH_2 protons. The ^1H NMR spectrum of the ligand, zinc and cadmium complexes were recorded to confirm the

binding of the Schiff base to the metal. There were no signals due to amine protons, confirming the complete synthesis of the Schiff base ligand. The Schiff base ligand (SI-26), HL shows a broad peak at 13.43 ppm due to the phenolic proton (-OH). A sharp peak at 8.28 ppm has been attributed to the azomethine proton (-N=CH-) of the Schiff base ligand, HL. The number of peaks in the ^{13}C NMR spectrum of HL (SI-27), and their chemical shifts, are also consistent with the ligand structure. Regarding ^{1}HNMR spectra, a comparison between the Zn and Cd complexes and the free Schiff base ligand (**2**) can be very useful. In fact, the lack of any signal for the phenolic groups (-OH) and also shifting of the peaks of the imine groups in the both Zn and Cd complexes compared to the free Schiff base ligand (**2**), indicates that these groups (phenolic and imine) are both coordinated to these metal atoms (phenolic group via oxygen and imine via nitrogen).[48] The imine resonance of the Cd complex at δ 8.16 ppm has two satellite peaks (3J~20 Hz for Cd–He) with intensities 1:6:1 due to coupling with neighboring $^{111/113}$Cd at natural abundance (^{111}Cd, 12.81; ^{113}Cd, 12.22%)[52]. The ^{13}C NMR spectra of the Zn and Cd complexes (SI-29 and 31) show peaks corresponding to the imine carbon atoms (155.50 ppm for the Zn and 148.48 ppm for the Cd). The signals related to the aromatic ring carbon atoms of the ligand and its complexes were determined to be in the region of 115-170 ppm.

3.7. Crystal structures

Crystal data are given in Table 1. The metal atoms in [ZnL](ClO_4) (**3**), [CdL](ClO_4) (**4**), and [CuL](ClO_4) (**7**) are each in a 5-coordinate environment, coordinated to the four nitrogen atoms and one oxygen atom of the pentacoordinate ligand; the presence of one non-coordinating perchlorate anion confirms that the phenol oxygen has been deprotonated. For all complexes, the M-O distance is significantly shorter than the M-N distances (Table 3). It can be seen that the

metal-ligand bond lengths follow the pattern M-$O2_{phenolic}$ < M-$N2_{imine}$ < M-$N4_{py}$ < M-$N1_{morpholine}$< M-$N3_{t\text{-}amine}$, except for the copper complex where the Cu-$N1_{morpholine}$ distance> Cu-$N3_{t\text{-}amine}$ distance. This is due to N1 being the apical position of the square pyramidal coordination environment where, in general, the copper apical-atom distance is greater than the distance from the copper atom to the atoms in the basal plane. The coordination geometry for all three structures are similar (Figs. 1-3). Continuous Shape Measure (CShM) calculations [53], and the Addison τ parameter [54], indicate that the coordination environments of the metal in these complexes lie between square pyramidal and trigonal bipyramidal (Table 4). The Cd and Zn complexes are best described as distorted trigonal bipyramidal, while the Cu complex is closer to a distorted square pyramidal structure. For the copper complex the oxygen and three nitrogen atoms (N2, N3, N4) lie in a distorted basal plane where the rms deviation from the least squares plane is 0.608 Å, with all atoms lying between 0.4278(12) Å and 0.7640(14) Å from the plane, and with the Cu atom lying 0.7770(10) Å out of this plane. The apical Cu-N bond length (Cu1-N1: 2.4430(18)Å) is much greater than the other Cu-N distances involving the equatorial atoms. For the zinc and cadmium complexes the metal atom is in a distorted trigonal bipyramidal environment, comprising N1, N2, N4 in the equatorial plane, with N3 and O1 being in the apical positions. The zinc and cadmium atoms lie 0.177(2) Å and 0.305(3) Å, respectively, above the trigonal plane, with both metal atoms being displaced towards N3. There is also a difference in the orientation of the salicylaldiminato moiety of the ligand for the Cd complex, compared to the Cu and Zn complexes, and the torsion angle N4-Cd1-O2-C22 is 118.1(5)°, compared to 155.40(19)° and 143.4(4)° for the corresponding torsion angles of the Cu and Zn complexes, respectively. Figure 4 and Figure 5 show the superposition of the three structures [55]; the greatest difference between the structures is due to the larger size of the Cd atom and the longer Cd-N

and Cd-O distances. For all three structures, weak C-H…O hydrogen bonds between the metal complex and the perchlorate anions link the moieties into a 3D network. These hydrogen bonds can be seen in the unit cell diagrams, which are shown in SI 32-34. The metal-ligand geometries found here are similar to those observed for some similar pentacoordinate N_3O_2 Zn Schiff base complexes [56] where the geometries lie between trigonal bipyramidal and square pyramidal and the metal- ligand bond lengths are in the order $M\text{-}O_{phenol} < M\text{-}N_{imine} < M\text{-}N_{py} < M\text{-}N_{t\text{-}amine}$.

Figs. 1-5 here

Table 3& 4 here

3.8. Cytotoxic activity

The cytotoxic potential of compounds **1-10** was evaluated using the MTT assay on MCF-7, MDA-MB-231 and PC-3 cancer cells, as well as WI-38 human normal lung fibroblast cells[36] [34]. IC_{50} values were defined as the concentration of compounds at which there was 50% growth inhibition of the cells and are shown in Table 5. Our results showed that all the compounds (except **1, 2** and **10**) have higher cytotoxicity potential towards breast cancer cells (MCF-7 and MDA-MB-231) than other types of cancer cells except for compound **8**. Compound **8** has shown a good cytotoxic activity towards prostate cancer cells. With respect to cisplatin, which is the commonly used chemotherapeutic drug, the results revealed that compound **4** and compound **8** possess better cytotoxic activity against MCF-7 and MDA-MB-231 breast cancer cells (higher than 3-times and nearly 3-times, respectively), but compound **5** showed similar activity towards MDA-MB-231 breast cancer cells (Table 5). It was found other compounds did not display any cytotoxic activity comparable with cisplatin.

Table 5 here

Figure **6** (**a-j**) shows the dose-dependent cytotoxic effect of compounds **1-10** on MCF-7, MDA-MB-231, PC-3 and WI-38 cells at 72 h. Compounds **1, 2** and **10** did not display any activity towards any cell line tested even at a concentration of 100 µM (Figures **6a, 6b, 6j**). It was observed that compounds were not cytotoxic towards the PC-3 cell line except for compound **8** (IC_{50}=28.5 µM, Figure **6h**). It was also determined that compound **4** and **8** have the highest cytotoxic activity towards the MCF-7, MDA-MB-231 cell lines (Figures **6d, 6h**). Compounds **3, 6** and **9** showed similar cytotoxic activity towards MCF-7, MDA-MB-231 and WI-38 cell lines (Figures **6c, 6f, 6i**). Since the compounds **3, 6** and **9** have similar IC_{50} values against cancer cells and normal cells, they have displayed poor selectivity between cancer cells and normal cells. According to our results, compound **5** showed different cytotoxic activity in all tested cell lines. IC_{50} values of compounds **5** were found to be 54.8 ± 0.08 µM, 26.5 ± 0.06 µM, >100 µM and 44.1 ± 0.04 µM against MCF-7, MDA-MB-231, PC-3 and WI-38 cell lines, respectively. The most important result was that compound 5 has lower cytotoxic activity against the WI-38 normal cell line according to the MDA-MB-231 cells and showed a selectivity index of approximately >2 for related cell lines.

Figure 6 here

Kaur and co-workers synthesized, characterized and evaluated the antimicrobial potential of a new series of morpholine based heterocyclic diazenyl chalcones [57]. They also investigated the cytotoxic activity of most active compounds against L929 mouse fibroblast cell line and the

A549 human lung cancer cell line. Novel pyrano[3,2-c]chromene derivatives bearing morpholine/phenylpiperazine moiety were synthesized and evaluated against acetylcholinestrase (AChE) and butylcholinestrase (BuChE) by Sameem and co-workers [58]. It was found that some of the compounds showed significant neuroprotective effects against H_2O_2-induced PC12 oxidative stress. In another study, researchers designed and synthesized a series of morpholine derivatives bearing chromone moiety (*tert*-Butyl, ethyl, isopropyl, methyl, hydroxy, fluoro, chloro, bromo) and evaluated their cytotoxicity against five cancer cell lines (A549, PC-3, MCF-7, Hela and Hep G2) by the standard MTT assay in vitro[58, 59]. They observed that seven of the target compounds (7,8-dihydro; *tert*-Butyl, ethyl, isopropyl, fluoro, 6-nitro, 4-oxo, 6,6-dioxido-; *tert*-Butyl) showed moderate to excellent cytotoxicity against the five tested cancer cell lines with IC_{50} values ranging from 34.9 to 0.17 µM, and most of them showed more activities against Hela and Hep G2 cancer cell lines than the other three cancer cell lines (A549, PC-3, MCF-7). They also found that compounds 7,8-dihydro; *tert*-Butyl and 6-hydroxy have weak cytotoxicity against the PC-3 prostate cancer cell lines with IC_{50} values > 100 µM while other compounds have moderate to good cytotoxic activity with IC_{50} values ranging from 14.3 to 83.9 µM. These results indicated that the substituent on the chromone moiety at the C-6 position played a key role in the cytotoxicity, with electron-donating groups (*tert*-Butyl, ethyl, isopropyl, methyl) being more cytotoxic than electron-withdrawing groups (hydroxy, fluoro, chloro, bromo). The results of the current study indicated that all complexes (except compound 8) have high IC_{50} values (> 100 µM) and showed weak cytotoxic activity similar to compounds 7,8-dihydro; *tert*-Butyl and 6-hydroxy. Morpholine is an important intermediate in many organic and industrial syntheses that are of great significance. Morpholine containing compounds have different biological activity. Gwaram and coworker

reported synthesis of some new synthesized *N'N''O* donor Schiff base ligands from the reaction of 4-(2-aminoethyl)morpholine with 2-hydroxyacetophenone and related metal complexes and activities of these compounds towards MCF-7 cells[56]. The metal complexes were found to inhibit the growth of MCF-7 cells in a dose-dependent manner. The MTT assay of the free ligand showed no significant inhibition activity while the metal complexes showed significant inhibition activities which confirmed that chelation of the ligand with metal ions was significant for the activity of these novel compounds. In another study, researchers synthesized some complexes of zinc featuring a heterocyclic amine and investigated their ability to enhance gastric self-repair [60]. They found that zinc-morpholine complex, Zn(L)SCN, exhibited anti-oxidative, anti-inflammatory and anti-apoptotic activities, all of which have cytoprotective effects on the gastric lining. In this work, the reason for the higher cytotoxic activity of compound **8** would be attributed to the silver centre.

4. CONCLUSION

In this work, we report the successful synthesis of some new N_4O Schiff base mononuclear complexes by condensation of a new branched amine, N1-(2-morpholinoethyl)-N1-((pyridine-2-yl)methyl)propane-1,3-diamine with 2-hydroxybenzaldehyde in the presence of various metal ions including Zn^{2+}, Cd^{2+}, Mn^{2+}, Cu^{2+}, Ni^{2+}, Ag^{+}, Fe^{3+} and Co^{2+}. These metal complexes were characterized by elemental analyses (only for C, H and N atoms), IR, ESI-MS, ^{1}H and ^{13}C NMR spectra (in the case of Cd and Zn complexes). The structure of the complexes, [ZnL](ClO_4) (**3**), [CdL](ClO_4) (**4**) and [CuL](ClO_4) (**7**) have been determined by single-crystal X-ray structural analysis, showing that the metal complexes have adopted distorted trigonal bipyramidal (Zn and Cd) or distorted square pyramidal (Cu) geometries. The cytotoxicity of these compounds was

evaluated using the MTT assay on MCF-7, MDA-MB-231 and PC-3 cancer cells, as well as WI-38 human normal lung fibroblast cells. Our results showed that all the compounds have higher cytotoxicity potential towards breast cancer cells (MCF-7 and MDA-MB-231) than other types of cancer cells except for compound **8**. Compound **8** has shown a good cytotoxic activity towards prostate cancer cells. A comparison between cisplatin, which is the commonly used chemotherapeutic drug, and our compounds revealed that compounds **4** and **8** possess better cytotoxic activity against MCF-7 and MDA-MB-231 breast cancer cells (higher than 3-times and nearly 3-times, respectively), while compound **5** shows similar activity towards MDA-MB-231 breast cancer cells. It has been found that other compounds did not have any activity comparable with cisplatin against all the cell lines. Moreover, it was observed that these compounds display different cytotoxic activities depending on concentration and cell line types. The most important result was that compound **5** displays different cytotoxic activities against different types of cell lines. For instance, it shows lower cytotoxicity against the WI-38 normal cell line than it does against the MDA-MB-231 cell line. All the results indicate that the activities of the synthesized compounds depend on the structural skeleton and electronic environment of the molecules, type of centre metal ions and cell line types.

Acknowledgments

We thank Hamedan University of Technology, Iran National Science Foundation (INSF) (grant no. 97005780) and University of Miami for financial support. Cytotoxic activity studies were done at Sivas Cumhuriyet University Advanced Technology Application and Research Center (SCUTAM).

Supplementary material

CCDC 1887832, 1887833 and 1887834 contain the supplementary crystallographic data for [ZnL](ClO_4), [CdL](ClO_4) and [CuL](ClO_4). Copies of this information may be obtained free of charge from The Director, CCDC,12 Union Road, Cambridge, CB21EZ, UK (fax:+44 1223 336033; mail:deposit@ccdc.cam.ac.uk).

References:

[1] G. Tantaru, M. C. Popescu, V. Bild, A. Poiata, G. Lisa, C. Vasile, *Appl Organomet Chem* **2012**, *26*, 356.
[2] R. D. Jones, D. A. Summerville, F. Basolo, *Chem Rev* **1979**, *79*, 139.
[3] J. Hernández-Gil, L. Perelló, R. Ortiz, G. Alzuet, M. Gonzalez-Alvarez, M. Liu-González, *Polyhedron* **2009**, *28*, 138.
[4] J. Margerum, L. Miller, Wiley, New York, **1971**.
[5] M. S. Babu, K. H. Reddy, P. G. Krishna, *Polyhedron* **2007**, *26*, 572.
[6] M. Rezaeivala, H. Keypour, *Coord Chem Rev* **2014**, *280*, 203.
[7] W. Al Zoubi, A. A. S. Al-Hamdani, M. Kaseem, *Appl Organomet Chem* **2016**, *30*, 810.
[8] K. Mjos, *Kirk-Othmer encyclopedia of chemical technology* **1978**, *2*, 298.
[9] M. Al-Ghorbani, A. B. Begum, M. S. Zabiulla, S. A. Khanum, *J. Chem. Pharm. Res* **2015**, *7*, 281.
[10] J. Knapp, V. Brown, *International biodeterioration* **1988**, *24*, 299.
[11] V. S. Mishra, J. B. Joshi, V. V. Mahajani, *Water Res* **1994**, *28*, 1601.
[12] J. E. Summerton, *Current topics in medicinal chemistry* **2007**, *7*, 651.
[13] V. Duhalde, B. Lahille, F. Camou, S. Pédeboscq, J. Pometan, *Pathol Biol (Paris)* **2007**, *55*, 478.
[14] H. Goudarziafshar, M. Rezaeivala, F. Khosravi, Y. Abbasityula, S. Yousefi, N. Özbek, V. Eigner, M. Dušek, *J IRAN CHEM SOC* **2015**, *12*, 113.
[15] S. Y. H. Goudarziafshar, Y. Abbasityula, M. Dusek, V. Eigner, M. Rezaeivala, N. Ozbeck, *CHINESE J INORG CHEM* **2015**, *31*, 1076.
[16] A. El-Sonbati, W. Mahmoud, G. G. Mohamed, M. Diab, S. M. Morgan, S. Abbas, *Appl Organomet Chem* **2019**, e5048.
[17] K. Dhahagani, S. M. Kumar, G. Chakkaravarthi, K. Anitha, J. Rajesh, A. Ramu, G. Rajagopal, *Spectrochim Acta A Mol Biomol Spectrosc* **2014**, *117*, 87.
[18] A. Aktaş, D. B. Celepci, R. Kaya, P. Taslimi, Y. Gök, M. Aygün, İ. Gülçin, *Polyhedron* **2019**, *159*, 345.
[19] F. Arshad, M. F. Khan, W. Akhter, M. M. Alam, L. M. Nainwal, S. K. Kaushik, M. Akhter, S. Parvez, S. M. Hasan, M. Shaquiquzzaman, *Eur. J. Med. Chem.* **2019**.
[20] V. Raparti, T. Chitre, K. Bothara, V. Kumar, S. Dangre, C. Khachane, S. Gore, B. Deshmane, *Eur. J. Med. Chem.* **2009**, *44*, 3954.
[21] P. Panneerselvam, R. R. Nair, G. Vijayalakshmi, E. H. Subramanian, S. K. Sridhar, *Eur. J. Med. Chem.* **2005**, *40*, 225.
[22] C. Manera, A. Martinelli, S. Nencetti, F. Romagnoli, A. Rossello, G. Giannaccini, R. Scatizzi, P. Cozzini, P. Domiano, *Eur. J. Med. Chem.* **1994**, *29*, 519.

[23] M. A. Ibrahim, S. M. Abou-Seri, M. M. Hanna, M. M. Abdalla, N. A. El Sayed, *Eur. J. Med. Chem.* **2015**, *99*, 1.

[24] K. Ohui, E. Afanasenko, F. Bacher, R. L. X. Ting, A. Zafar, N. r. Blanco-Cabra, E. Torrents, O. Dömötör, N. r. V. May, D. Darvasiova, *J. Med. Chem.* **2018**, *62*, 512.

[25] M. Rezaeivala, R. Golbedaghi, M. Khalili, M. Ahmad, K. Sayin, F. Chalabian, *RUSS J COORD CHEM* **2019**, *45*, 142.

[26] H. Keypour, A. Shooshtari, M. Rezaeivala, M. Bayat, H. A. Rudbari, *Inorg. Chim. Acta* **2016**, *440*, 139.

[27] M. Rezaeivala, S. Salehzadeh, H. Keypour, S. W. Ng, L. Valencia, *Arab. J. Chem.* **2016**, *9*, S1610.

[28] S. Kalhor, M. Yarie, M. Rezaeivala, M. A. Zolfigol, *RES CHEM INTERMEDIAT* **2019**, *45*, 3453.

[29] A. Version, *Inc., Madison, Wisconsin, USA* **2007**.

[30] G. M. Sheldrick, *Acta Crystallogr A* **2008**, *64*, 112.

[31] G. M. Sheldrick, *Acta Crystallogr C Struct Chem* **2015**, *71*, 3.

[32] H. Keypour, M. Ahmadi, M. Rezaeivala, A. Chehregani, R. Golbedaghi, A. G. Blackman, *Polyhedron* **2011**, *30*, 1865.

[33] M. Rezaeivala, H. Keypour, S. Salehzadeh, R. Latifi, F. Chalabian, F. Katouzian, *J IRAN CHEM SOC* **2014**, *11*, 431.

[34] P. Skehan, R. Storeng, D. Scudiero, A. Monks, J. McMahon, D. Vistica, J. T. Warren, H. Bokesch, S. Kenney, M. R. Boyd, *J NATL CANCER I* **1990**, *82*, 1107.

[35] W. J. Geary, *Coord Chem Rev* **1971**, *7*, 81.

[36] E. Tas, M. Aslanoglu, A. Kilic, O. Kaplana, H. Temel, *J. Chem. Res.* **2006**, *2006*, 242.

[37] E. Sinn, C. M. Harris, *Coord Chem Rev* **1969**, *4*, 391.

[38] A. Prakash, R. Malhotra, *Appl Organomet Chem* **2018**, *32*, e4098.

[39] H. Keypour, M. Shayesteh, M. Rezaeivala, F. Chalabian, Y. Elerman, O. Buyukgungor, *J. Mol. Struct.* **2013**, *1032*, 62.

[40] H. Keypour, M. Shayesteh, M. Rezaeivala, F. Chalabian, L. Valencia, *Spectrochim Acta A Mol Biomol Spectrosc* **2013**, *101*, 59.

[41] M. Tyagi, S. Chandra, P. Tyagi, *Spectrochim Acta A Mol Biomol Spectrosc* **2014**, *117*, 1.

[42] M. G. Bhowon, H. Li Kam Wah, A. Dosieah, M. Ridana, O. Ramalingum, D. Lacour, *SYNTH REACT INORG M* **2004**, *34*, 1.

[43] T. A. Khan, M. A. Rather, N. Jahan, S. P. Varkey, M. Shakir, *SYNTH REACT INORG M* **1997**, *27*, 843.

[44] H. Keypour, M. Rezaeivala, L. Valencia, P. Pérez-Lourido, H. R. Khavasi, *Polyhedron* **2009**, *28*, 3755.

[45] A. P. Lever, E. Mantovani, B. Ramaswamy, *Can J Biochem* **1971**, *49*, 1957.

[46] B. Hathaway, A. Underhill, *J. Chem. Soc.* **1961**, 3091.

[47] M. R. Rosenthal, *J. Chem. Educ.* **1973**, *50*, 331.

[48] Y.-J. Sun, Q.-Q. Huang, T. Tano, S. Itoh, *Inorg Chem* **2013**, *52*, 10936.

[49] F. Ahmad, M. Parvez, S. Ali, M. Mazhar, A. Munir, *SYNTH REACT INORG M* **2002**, *32*, 665.

[50] S. S. Massoud, L. Le Quan, K. Gatterer, J. H. Albering, R. C. Fischer, F. A. Mautner, *Polyhedron* **2012**, *31*, 601.

[51] P. J. Desrochers, R. W. Cutts, P. K. Rice, M. L. Golden, J. B. Graham, T. M. Barclay, A. Cordes, *Inorg Chem* **1999**, *38*, 5690.

[52] H. Keypour, M. Rezaeivala, L. Valencia, S. Salehzadeh, P. Pe, H. R. Khavasi, *Polyhedron* **2009**, *28*, 3533.

[53] S. Alvarez, P. Alemany, D. Casanova, J. Cirera, M. Llunell, D. Avnir, *Coord Chem Rev* **2005**, *249*, 1693.

[54] A. Addison, *J. Chem. Soc., Dalton. Trans* **1984**, *1349*.

[55] N. S. Gwaram, P. Hassandarvish, *J App Pharm Sci* **2014**, *4*, 75.

[56] S. M. Salama, N. S. Gwaram, A. S. AlRashdi, S. A. Khalifa, M. A. Abdulla, H. M. Ali, H. R. El-Seedi, *Sci. Rep.* **2016**, *6*, 29646.
[57] H. Kaur, S. D. Desai, J. Singh, B. Narasimhan, *ANTI-CANCER AGENT ME* **2018**, *18*, 2193.
[58] B. Sameem, M. Saeedi, M. Mahdavi, H. Nadri, F. H. Moghadam, N. Edraki, M. I. Khan, M. Amini, *Bioorg Med Chem* **2017**, *25*, 3980.
[59] C. Sun, C. Chen, S. Xu, J. Wang, Y. Zhu, D. Kong, H. Tao, M. Jin, P. Zheng, W. Zhu, *Bioorg Med Chem* **2016**, *24*, 3862.
[60] H. Keypour, M. Shayesteh, M. Rezaeivala, S. Dhers, K. Sayin, *Inorg. Chim. Acta* **2018**, *473*, 94.
[61] D. Iacopetta, A. Mariconda, C. Saturnino, A. Caruso, G. Palma, J. Ceramella, N. Muià, M. Perri, M. S. Sinicropi, M. C. Caroleo, *ChemMedChem* **2017**, *12*, 2054.
[62] S. Jaeger, L. Gude, M.-S. Arias-Perez, *Bioorg. Chem.* **2018**, *81*, 405.
[63] M. Napoli, C. Saturnino, E. Sirignano, A. Popolo, A. Pinto, P. Longo, *Eur. J. Med. Chem.* **2011**, *46*, 122.
[64] Y. Zhou, T. Song, Y. Cao, G. Gong, Y. Zhang, H. Zhao, G. Zhao, *J. Organomet. Chem.* **2018**, *871*, 1.

Table 1. Crystallographic Data for Compounds [ZnL](ClO_4)(3), [CdL](ClO_4)(4), [CuL](ClO_4)(7).

	(3)	(4)	(7)
Empirical formula	$C_{22}H_{29}ClN_4O_6Zn$	$C_{22}H_{29}ClN_4O_6Cd$	$C_{22}H_{29}ClN_4O_6Cu$
Formula weight	546.31	593.34	544.48
Crystal system	Orthorhombic	Orthorhombic	Orthorhombic
Lattice parameters			
a (Å)	10.9912(3)	11.0542(7)	8.9981(3)
b (Å)	14.1953(5)	14.2608(9)	13.9147(5)
c (Å)	15.6528(5)	15.6007(10)	18.6984(7)
V (Å^3)	2442.20(13)	2459.3(3)	2341.15(14)
Space group	$P2_12_12_1$ (# 19)	$P2_12_12_1$ (# 19)	$P2_12_12_1$ (# 19)
Z value	4	4	4
ρ_{calc} (g / cm^3)	1.486	1.602	1.545
μ (Mo Kα) (mm^{-1})	1.160	1.041	1.094
Temperature (K)	294	294	294
$2\Theta_{max}$ (°)	57.96	56.00	59.58
No. Obs. (I > 2σ(I))	5714	4671	5806
No. Parameters	308	308	308
Goodness of fit	1.022	1.032	1.025
Max. shift in cycle	0.001	0.000	0.001
Residuals*:R1; wR2	0.0359; 0.1041	0.0408; 0.0955	0.0315; 0.0812
Absorption Correction, Max/min	Multi-scan 0.7462/0.6265	Multi-scan 0.7457/0.6773	Multi-scan 0.7459/0.6300
Largest peak in Final Diff. Map (e$^-$ / Å^3)	0.675	0.536	0.589

*$R1 = \Sigma_{hkl}(\,|\,|F_{obs}|-|F_{calc}|\,|)/\Sigma_{hkl}|F_{obs}|$; $wR2 = [\Sigma_{hkl}w(|F_{obs}|-|F_{calc}|)^2/\Sigma_{hkl}wF_{obs}^2]^{1/2}$, $w = 1/\sigma^2(F_{obs})$; $GOF = [\Sigma_{hkl}w(|F_{obs}|-|F_{calc}|)^2/(n_{data} - n_{vari})]^{1/2}$.

Table 2. The characteristic infrared absorptions of ligand and their metal complexes

Compound	υ (O-H)	υ (N-H)	υ (C-H)	υ $(C=N)_{im}$	υ $(C=N)_{py}$	υ (C-C)	υ (C-N)	υ (C-O)	υ (Cl-O)	υ (M-N)	υ (M-O)
(1)	-	3284, 3357	2950	-	1591	1472	1117	-	-	-	-
HL(2)	3397	-	2952	1632	1598	1459	1117	1280	-	-	-
$[ZnL](ClO_4)$	-	-	2974	1618	1578	1474	1143	1243	1088, 626	589	464
$[CdL](ClO_4)$	-	-	2974	1616	1601	1442	1145	1248	1088, 627	593	474
$[MnL](ClO_4)$	-	-	2953	1622	1573	1446	1146	1256	1091, 624	572	471
$[CuL](ClO_4)$	-	-	2975	1619	1540	1444	1198	1249	1090, 625	590	469
$[NiL](ClO_4)$	-	-	2936	1617	1535	1439	1147	1260	1089, 626	574	472
$[AgHL](NO_3)$	3448	-	2966	1633	1602	1456	1114	1299	-	571	-
$[FeLCl_2]$	-	-	2945	1627	1610	1467	1118	1266	-	574	470
$[CoL](ClO_4)$	-	-	2950	1613	1585	1450	1114	1245	1090, 624	587	467

Table 3. Selected Bond Lengths (Å) and Angles (°) for complexes

	[ZnL](ClO$_4$)	**[CdL](ClO$_4$)**	**[CuL](ClO$_4$)**
M-O2	1.979(3)	2.164(5)	1.905(19)
M-N1	2.131(3)	2.305(4)	2.442(2)
M-N2	2.039(3)	2.215(5)	1.984(2)
M-N3	2.247(3)	2.382(5)	2.093(2)
M-N4	2.106(3)	2.304(5)	2.032(2)
O2-M-N2	91.47(11)	87.1(2)	93.67(9)
O2-M-N3	167.23(13)	168.4 (2)	168.33(9)
O2-M-N4	91.13(12)	98.9(2)	88.37(9)
O2-M-N1	103.58(12)	109.99(19)	97.09(9)
N2-M-N3	93.25(12)	91.8(2)	97.68(10)
N2-M-N4	133.15(12)	128.08(18)	151.89(10)
N2-M-N1	118.25(11)	125.69(19)	107.96(9)
N3-M-N4	77.00(12)	72.8 (2)	80.35(9)
N3-M-N1	84.57(11)	79.92(19)	81.99(8)
N4-M-N1	106.44(11)	100.65(18)	99.57(8)
N4-M-O2-C5	127.50(3)	118.10(6)	155.0(2)
N4-M-N2-C11	-85.20(3)	-88.80(6)	-91.80(3)

Table 4. Metal ligand geometry Shape parameters.

Parameter	**[ZnL](ClO$_4$)**	**[CdL](ClO$_4$)**	**[CuL](ClO$_4$)**
TBPY-5	1.612	1.978	2.472
SPY-5	2.281	3.730	1.972
τ5	0.491	0.668	0.274

$\tau_{5=}(\beta - \alpha)/60$. $\tau_{5=}0$: square pyramidal, $\tau_{5=}1$: trigonal pyramidal.

Table 5. Cytotoxic activities [a] of compounds **1-10** on MCF-7, MDA-MB-231, PC-3 and WI-38 cells

Compound	MCF-7[b]	MDA-MB-231[b]	PC-3[b]	WI-38[c]
1	>100	>100	>100	>100
2	>100	>100	>100	>100
3	72.1 ± 0.07	84.5 ± 0.06	>100	60.7 ± 0.08
4	<10	<10	>100	<10
5	54.8 ± 0.08	26.5 ± 0.06	>100	44.1 ± 0.04
6	67.5 ± 0.11	75.2 ± 0.07	>100	69.9 ± 0.10
7	90.9 ± 0.05	69.0 ± 0.07	>100	15.45 ± 0.03
8	10.9 ± 0.03	10.2 ± 0.06	28.5 ± 0.30	<10
9	90.5 ± 0.07	81.8 ± 0.06	>100	>100
10	>100	>100	>100	>100
Cisplatin	35.8 ± 1.3[61] 33.7[63]	28.7 ± 1.0[61] 33.7 ± 15.2[64]	12.8 ± 0.9[62]	

[a]Cell viability after treatment for 72 h was determined by MTT staining as described in the Experimental section (μM). [b] Cancer cells, [c] Normal cells. The cisplatin is a standard drug. Each IC_{50} value represents the mean ± SEM of three independent experiments (nine replicates).

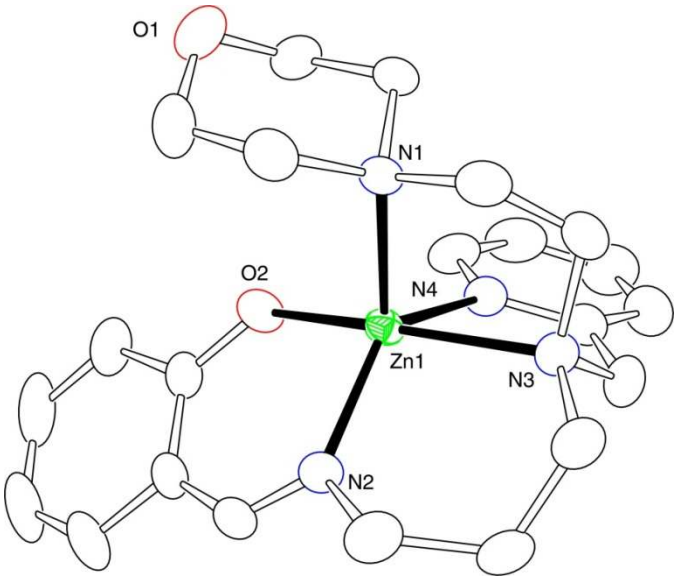

AOC_5325_F1.tif

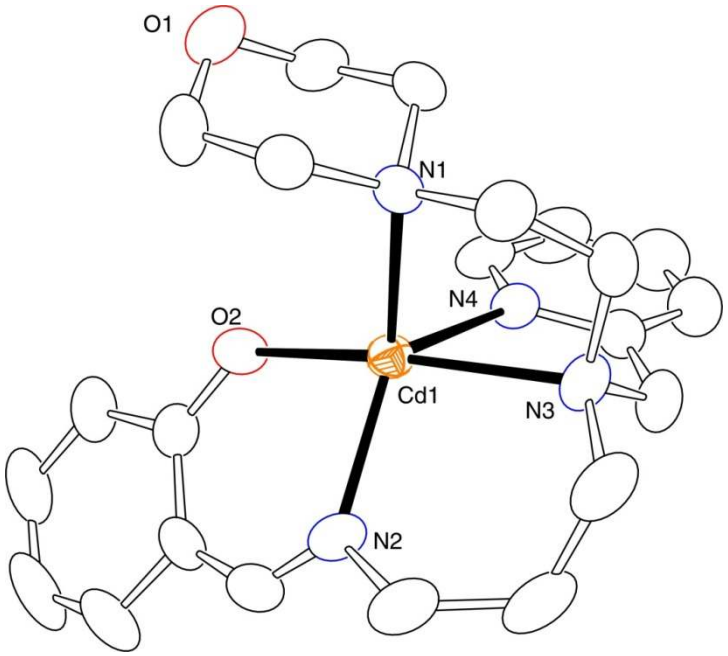

AOC_5325_F2.tif

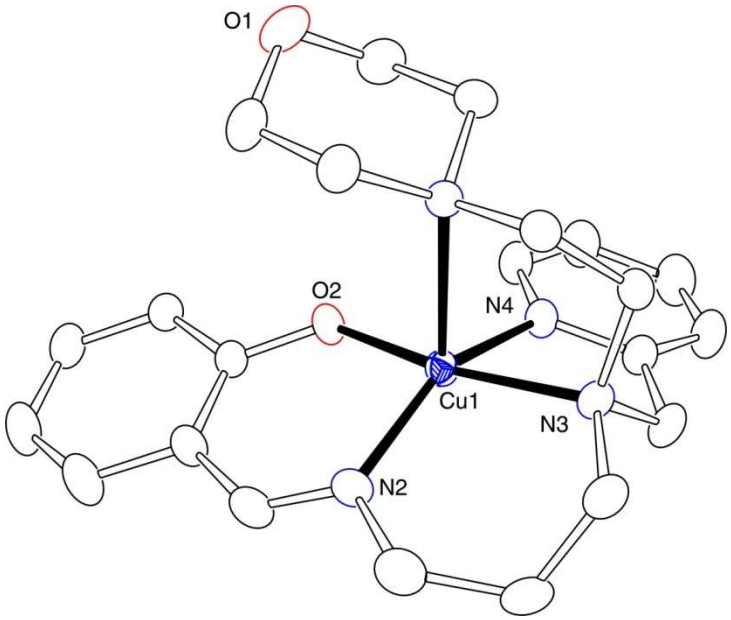

AOC_5325_F3.tif

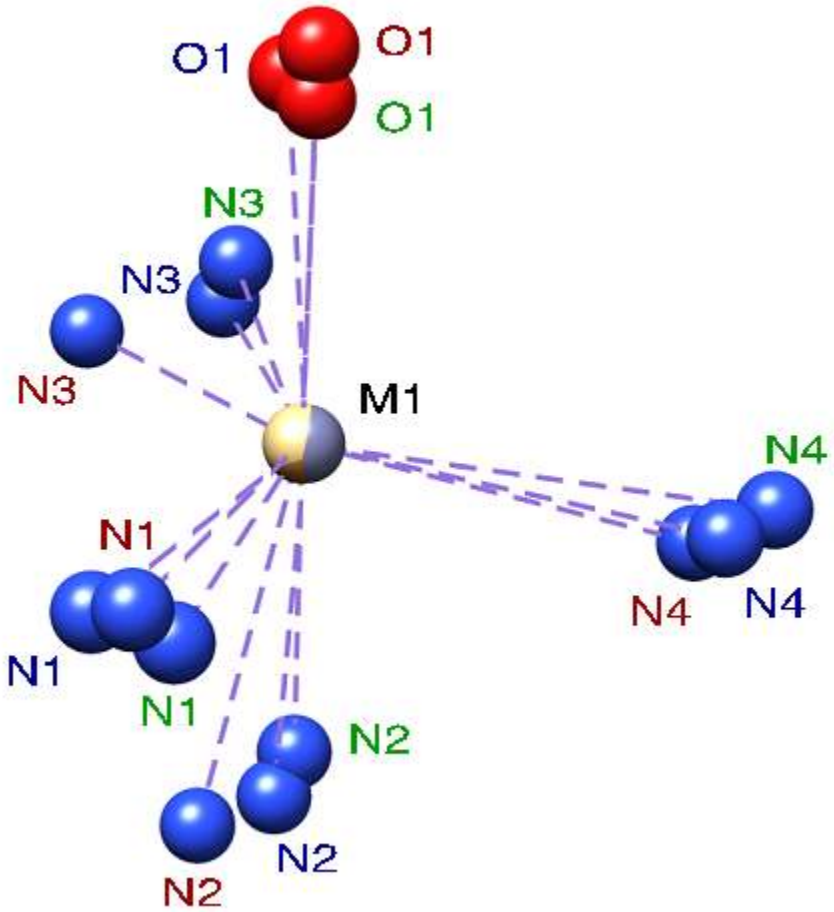

AOC_5325_F4.tif

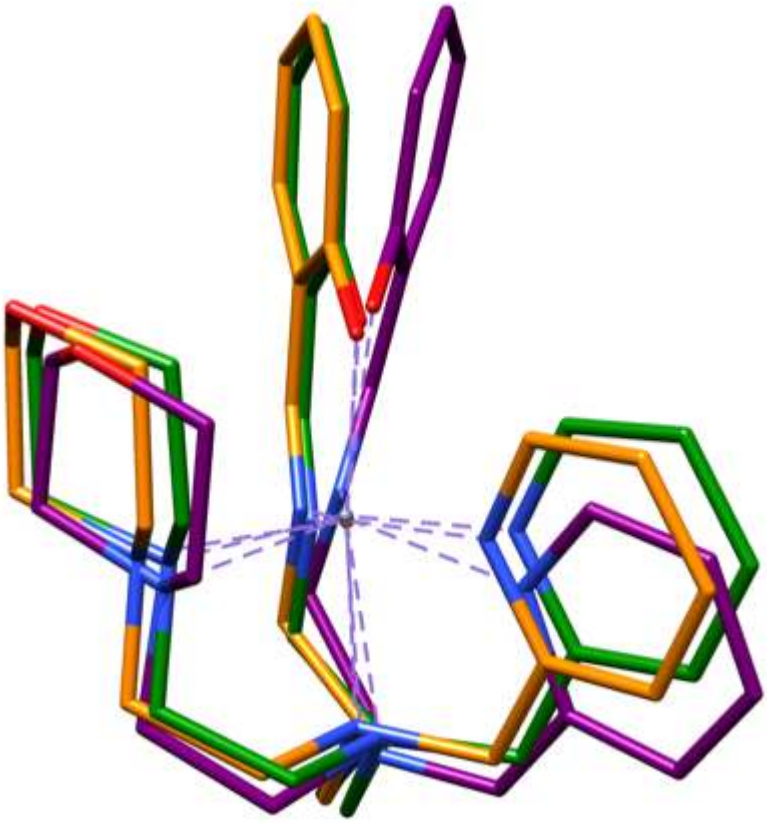

AOC_5325_F5.tif

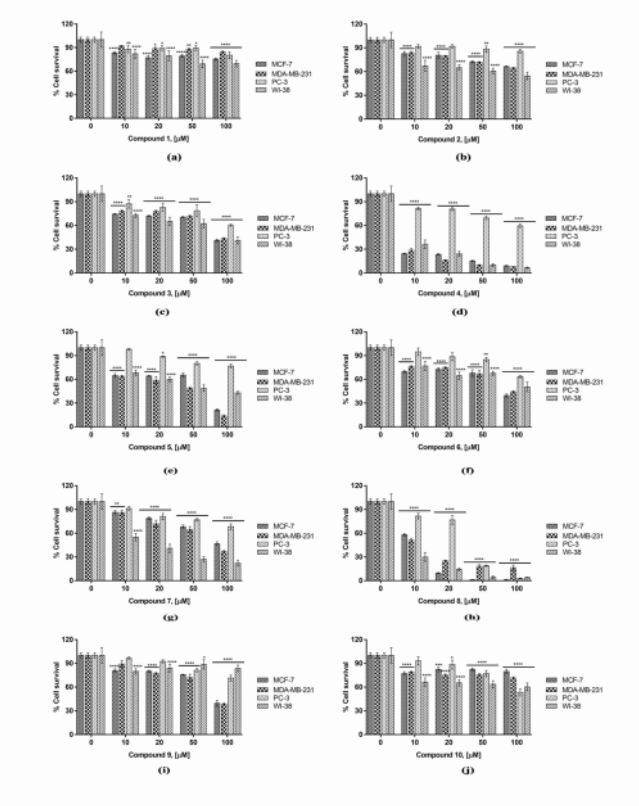

AOC_5325_F6.tif

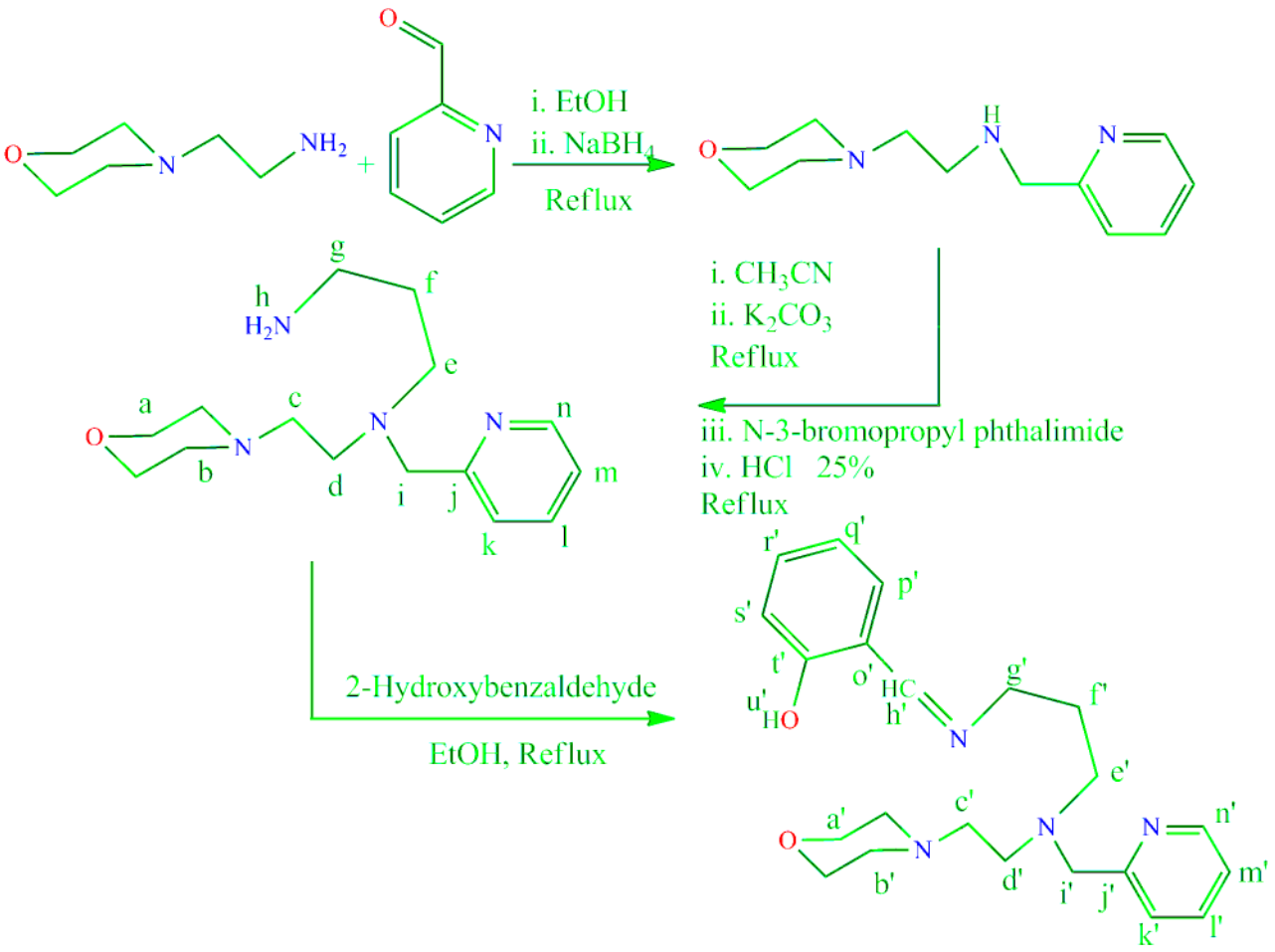

AOC_5325_scheme1.tif

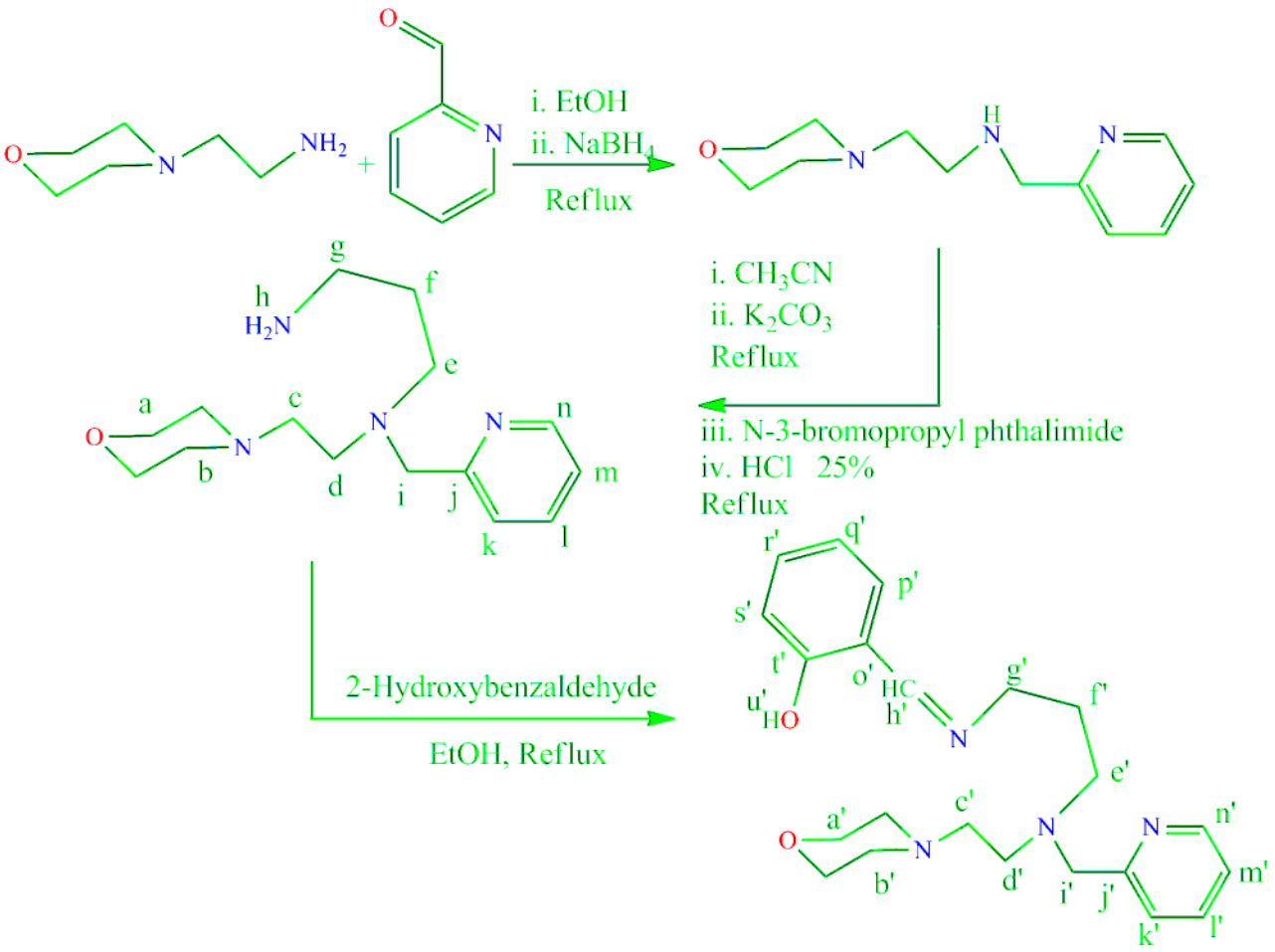

AOC_5325_Scheme 1.tif

Author/s:
Rezaeivala, M;Ahmadi, M;Captain, B;Sahin-Bolukbasi, S;Dehghani-Firouzabadi, AA;Gable, RW

Title:
Synthesis, characterization, and cytotoxic activity studies of new N4O complexes derived from 2-({3-[2-morpholinoethylamino]-N3-([pyridine-2-yl]methyl) propylimino} methyl)phenol

Date:
2019-12-20

Citation:
Rezaeivala, M., Ahmadi, M., Captain, B., Sahin-Bolukbasi, S., Dehghani-Firouzabadi, A. A. & Gable, R. W. (2019). Synthesis, characterization, and cytotoxic activity studies of new N4O complexes derived from 2-({3-[2-morpholinoethylamino]-N3-([pyridine-2-yl]methyl) propylimino} methyl)phenol. APPLIED ORGANOMETALLIC CHEMISTRY, 34 (2), https://doi.org/10.1002/aoc.5325.